Design, semi-synthesis and examination of new gypsogenin derivatives against leukemia via Abl tyrosine kinase inhibition and apoptosis induction

Nafia Gökçe Ulusoy, Safiye Emirdağ, Ece Sözer, Mohamed O. Radwan, Halilibrahim Çiftçi, Mehran Aksel, Serap Şahin Bölükbaşı, Ali Özmen, Nurettin Yaylı, Tamer Karayıldırım, Özgen Alankuş, Hiroshi Tateishi, Masami Otsuka, Mikako Fujita, Belgin Sever

PII: S0141-8130(22)02196-1

DOI: https://doi.org/10.1016/j.ijbiomac.2022.09.257

Reference: BIOMAC 22132

To appear in: *International Journal of Biological Macromolecules*

Received date: 22 June 2022

Revised date: 19 September 2022

Accepted date: 28 September 2022

Please cite this article as: N.G. Ulusoy, S. Emirdağ, E. Sözer, et al., Design, semi-synthesis and examination of new gypsogenin derivatives against leukemia via Abl tyrosine kinase inhibition and apoptosis induction, *International Journal of Biological Macromolecules* (2022), https://doi.org/10.1016/j.ijbiomac.2022.09.257

Design, semi-synthesis and examination of new gypsogenin derivatives against leukemia via Abl tyrosine kinase inhibition and apoptosis induction

Nafia Gökçe Ulusoy[a], Safiye Emirdağ[a,*], Ece Sözer[a], Mohamed O. Radwan[b,c], Halilibrahim Çiftçi[b,d,e], Mehran Aksel[f], Serap Şahin Bölükbaşı[g], Ali Özmen[h], Nurettin Yaylı[i], Tamer Karayıldırım[a], Özgen Alankuş[a], Hiroshi Tateishi[b], Masami Otsuka[b,d], Mikako Fujita[b], Belgin Sever[b,j,*]

[a] *Chemistry Department, Faculty of Science, Ege University, Izmir, 35040, Turkey*

[b] *Medicinal and Biological Chemistry Science Farm Joint Research Laboratory, Faculty of Life Sciences, Kumamoto University, 5-1 Oe-honmachi, Chuo-ku, Kumamoto 862-0973, Japan*

[c] *Chemistry of Natural Compounds Department, Pharmaceutical and Drug Industries Research Division, National Research Centre, Dokki 12622, Cairo, Egypt*

[d] *Department of Drug Discovery, Science Farm Ltd., 1-7-30-805 Kuhonji, Chuo-ku, Kumamoto 862-0976, Japan*

[e] *Department of Molecular Biology and Genetics, Koc University, Istanbul 34450, Turkey*

[f] *Department of Biophysics, Faculty of Medicine, Adnan Menderes University, Aydin, 09010, Turkey*

[g] *Department of Biochemistry, Faculty of Pharmacy, Afyonkarahisar Health Sciences University, Afyon, Turkey*

[h] *Department of Medical Biology, Faculty of Medicine, Adnan Menderes University, Aydin, 09010, Turkey*

[i] *Faculty of Pharmacy, Karadeniz Technical University, Trabzon 61080, Turkey*

[j] Department of Pharmaceutical Chemistry, Faculty of Pharmacy, Anadolu University, Eskisehir 26470, Turkey

* Corresponding author. *E-mail address:* emirdagsafiye@gmail.com (S. Emirdağ);

belginsever@anadolu.edu.tr (B. Sever)

ABSTRACT

Chronic myelogenous leukemia (CML) is characterized by Philadelphia translocation arising from Bcr-Abl fusion gene, which encodes abnormal oncoprotein showing tyrosine kinase (TK) function. Certain mutations in kinase domain, off-target effects and resistance problems of current TK inhibitors require the discovery of novel Abl TK inhibitors. For this purpose, herein, we synthesized new gypsogenin derivatives (**6a-l**) and evaluated their anticancer effects towards CML cells along with healthy cell line and different leukemic cells. Among these compounds, compound **6l** was found as the most active anti-leukemic agent against K562 CML cells compared to imatinib exerting less cytotoxicity towards PBMCs (healthy). This compound also revealed significant anti-leukemic effects against Jurkat cell line. Besides, compound **6l** enhanced apoptosis in CML cells with 52.4% when compared with imatinib (61.8%) and inhibited Abl TK significantly with an IC_{50} value of 13.04± 2.48 μM in a large panel of kinases accentuating Abl TK-mediated apoptosis of compound **6l** in CML cells. Molecular docking outcomes showed that compound **6l** formed mainly crucial interactions in the ATP-binding cleft of Abl TK similar to that of imatinib. Ultimately, *in silico* pharmacokinetic evaluation of compound **6l** indicated that this compound was endowed with anti-leukemic drug candidate features.

Keywords*:* Chronic myelogenous leukemia, Abl tyrosine kinase, Apoptosis, Gypsogenin derivatives, Imatinib, Molecular docking

1. Introduction

Chronic myeloid leukemia (CML), a myeloproliferative disease, is related to malignant transformation of mature and maturing granulocytes and existence of Philadelphia chromosome originating from a translocation leading to the abnormal fusion of the Abelson oncogene (Abl) with the breakpoint cluster region (Bcr) gene, which turn translates into Bcr-

Abl, a fundamentally active tyrosine kinase (TK) [1, 2].

The Bcr-Abl oncoprotein displays the same kinase activity but different proliferative activity with the progenitor Abl, which has important roles in the regulation of several antiapoptotic and proliferative signal transduction pathways [3]. Two distinct groups of Abl TK are known namely, c-Abl and v-Abl. The first of these is responsible for reorganization of the cytoskeleton following DNA damage and oxidative stress [4].

In recent years, targeted therapies have got the edge over cytotoxic therapies due to better cure rates and lower toxicity profiles acting on specific molecular targets. The recognition of Bcr-Abl oncoprotein has led to the design and development of imatinib (Fig. 1A), the first approved targeted therapy in CML as an important Abl TK inhibitor [5]. Imatinib shows its effects binding to ATP-binding pocket of the Abl TK thus preventing Bcr-Abl autophosphorylation and substrate phosphorylation and eventually proliferation and impair of apoptosis [6,7].

In spite of being a milestone in current CML treatment with high remission rates, less side effects and considerably enhanced patient survival, the treatment with imatinib fails to achieve a satisfactory therapeutic effect owing to occurrence of resistance generally stemming from mutations in the TK domain of Bcr-Abl protein [8, 9]. Therefore, second and third generation of TK inhibitors including dasatinib, nilotinib, bosutinib and ponatinib (Fig. 1A) were introduced for patients who struggle with imatinib tolerance [10]. However, these compounds also target the TK domain of the Bcr-Abl protein with a distinct affinity under the particular mutations in the TK domain resulting in specific toxicity leading to treatment discontinuation [11]. These resistance and toxicity problems require the discovery of new Abl TK inhibitors to be efficient in CML treatment.

Natural products have been reported to serve as prominent Bcr-Abl inhibitors. Curcumin, radicicol, emodin, α-mangostin, genistein and homoharringtonine were found to

control or diminish Bcr-Abl levels in CML cells (Fig. 1B) [12, 13].

Apart from these compounds, saponins are bioactive compounds that include an aglycone-bound moiety. Due to pharmacological effects of saponins, they have always attracted great attention. In particular, it was reported that saponins from the roots of the *Gypsophila* species exhibited a wide range of activities including antimicrobial and antioxidant properties [14-16].

More studies also showed how saponins (separated into two major classes: triterpenoid and steroid glycosides) played important roles in the various applications from use in industry as household detergents to control microbial spoilage in food as well as natural surfactant [17,18]. Therefore, the roots that contain rich saponins of the *Gypsophila* species constitute a valuable source. These triterpenoid saponins can be extracted from *Gypsophila*, a genus of *Caryophyllaceae* family [19,20].

Gypsogenin (Fig. 1B), a natural saponin, can be obtained boiling roots from *Gypsophila arrostii*. In previous studies, the anticancer effects of gypsogenin aglicon and its derivatives on leukemia, glioma, lung, liver, gastric, colorectal, ovary and cervical cancer cell lines have been reported [21-27]. Besides, our research team also determined that gypsogenin derivatives exhibited notable anti-leukemic effects *via* the Abl TK inhibition [28, 29]. In these studies, the anticancer effects of compounds **1c** [28] and **GP2** and **GP5** [29] were found significant on CML cells. Compounds **1c** and **GP2** and **GP5** (Fig. 2) exerted their anti-leukemic activity through strong Abl TK inhibition with IC_{50} values of 8.7 µM, 7.19 µM and 6.16 µM, respectively.

In the light of the enriched literature, in this current work, we reported the semi-synthesis of new compounds (**6a-l**) from starting gypsogenin and evaluated their anticancer activity against CML cell line along with other leukemia and cervical cancer cells and healthy cell line to determine its selective cytotoxicity profile on CML cells. The mechanistic anti-

leukemic effects of the most promising derivative were explored *via* the detection of its apoptotic activity on CML cells and Abl TK inhibitor effects. Moreover, this derivative was further evaluated for its inhibitory activity on fifteen divergent tyrosine kinases. Molecular docking study was conducted for these derivatives in the ATP-binding pocket of Abl TK to find out its binding affinity and interactions. Drug-like properties were also ascertained for these derivatives by *in silico* pharmacokinetic studies.

2. Results and Discussion

2.1. Chemistry

The semi-synthesis of new gypsogenin derivatives (**6a-l**) bearing different amine structures was performed as depicted in Scheme 2. Compound **1** (gypsogenin), was achievable starting from the commercially available boiling water extract of *Gypsophila arrostii* roots and its isolation has been given in our previous study [22] (Scheme 1). In the first modification, the gypsogenin-derived compounds were synthesized for the first time starting from gypsogenin aglicon. Different amine and aniline derivatives were used for desired new gypsogenin-amine derivatives (**6a-l**) (Scheme 2).

Reductive amination of the carbonyl compounds or reductive alkylations of the amines is a very useful method to afford different amines. In these type of reactions 1,2-dichloroethane is the preferred reaction solvent and sodium triacetoxyborohydride gave consistently higher yields and fewer side products compare to other reductive amination procedures [30, 31].

These new derivatives were semi-synthesized by the treatment of different amine compounds and substituted phenyl amine derivatives with starting material (compound **1** (gypsogenin)). Initially, compound **1** was treated with amine derivatives in the presence of 1,2-dichloroethane subsequently with $NaBH(OAc)_3$ to obtain new semi-synthesized compounds (**6a-l**) in good yields (Scheme 2).

2.2. Spectral analysis

The structures of title compounds **6a-l** were elucidated by different spectroscopic techniques, such as infrared spectra (IR), ^{1}H nuclear magnetic resonance (NMR), ^{13}C NMR and LC-MS. The diagram for the spectral analysis was outlined in Fig. 3. In the ^{1}H NMR spectra of compounds **6a-l**, the characteristic peaks of H-3, H-12, H-18, H-23, H-24, H-25, H-26, H-27, H-29 and H-30 appeared at 3.05-4.11 ppm, 5.06-5.14 ppm, 2.70-3.40 ppm, 3.03-4.35 ppm, 0.48-0.92 ppm, 0.63-0.93 ppm, 0.67-0.91 ppm, 0.83-1.20 ppm, 0.83-1.85 ppm and 0.81-1.05 ppm, respectively. The absence of aldehyde proton and the observation of the protons of substituents of each compound at appropriate region confirmed the structures of final compounds. Besides, in the ^{13}C NMR spectra of compounds **6a-l**, the characteristic peaks of C-1, C-2, C-3, C-4, C-5, C-6, C-7, C-8, C-9, C-10, C-11, C-12, C-13, C-14, C-15, C-16, C-17, C-18, C-19, C-20, C-21, C-22, C-23, C-24, C-25, C-26, C-27, C-29 and C-30 were detected at 37.8-38.3 ppm, 15.3-27.6 ppm, 70.3-78.3 ppm, 39.1-65.7 ppm, 47.5-59.9 ppm, 13.5-18.3 ppm, 32.0-36.7 ppm, 38.0-39.2 ppm, 45.8-47.2 ppm, 36.4-38.1 ppm, 19.3-23.8 ppm, 120.9-122.3 ppm, 143.8-144.5 ppm, 41.7-45.8 ppm, 17.7-30.9 ppm, 22.8-28.4 ppm, 46.0 ppm, 39.0-41.5 ppm, 42.3-48.9 ppm, 30.2-36.7 ppm, 33.4-39.3 ppm, 32.4-38.3 ppm, 51.2-65.8 ppm, 9.8-13.1 ppm, 11.1-27.6 ppm, 12.8-25.7 ppm, 16.3-26.1 ppm, 15.8-33.3 ppm and 14.8-33.0 ppm, respectively. The presence of carboxylic acid carbon peaks at 178.3-196.0 ppm, the absence of aldehyde carbon peak and the observation of carbon peaks of substituents of compounds **6a-l** substantiated the formation of the final compounds along with the IR and LC-MS data of compounds **6a-l**.

2.3. Biological evaluation

CML is a malignant myeloproliferative neoplasm that accounts for approximately 20% of all cases of leukemia in adults. Despite the understanding of the molecular etiology of CML and the advancements in the new therapeutic options, the prognosis of patients with

CML still remains dismal [32, 33].

Natural products are considered as a rich source for the development of new therapeutic candidates, in particular for anti-cancer drug development that 25% of all newly approved anticancer drugs have been associated with natural products in very recent years. However, some difficulties to obtain new agents from natural sources such as identification and large-scale isolation have changed the direction of the major pharmaceutical companies to chemically synthesized compounds [34, 35]. Semi-synthesis is one of the most acceptable and useful methods to transform bioactive natural compounds to more effective analogues [36]. Omacetaxine is a very good example of that as a semi-synthetic form of homoharringtonine (Fig. 1B) and it has been approved for the treatment of CML refractory to TK inhibitors [37].

In a similar manner, our previous encouraging results about anti-leukemic potential of gypsogenin derivatives [28, 29] guided us to investigate antiproliferative activity of semi-synthetic new gypsogenin derivatives. Initially, new compounds (**6a-l**) were analyzed for their cytotoxic potential on K562 CML cells using MTT assay. According to the results, compound **6l** showed the most potential anti-leukemic properties in this series with an IC_{50} value of 11.32 ± 2.04 μM compared to control drug imatinib (IC_{50}= 4.89 ± 1.86 μM). On the other hand, this compound exhibited high selectivity (Selectivity Index (SI)= 3.59) between K562 CML and human peripheral blood mononuclear cells (PBMCs) (healthy) compared to imatinib (SI= 5.26) (Table 1). This finding pointed that the 4-(methylphenyl)amino moiety enhanced selective anti-leukemia activity in gypsogenin framework. Apart from compound **6l,** it was found that the cytotoxic potency order of the gypsogenin derivatives against K562 cell line was: compound **6j** > compound **6a** > compound **6k** > compound **6e** > compound **6b**. The IC_{50} values of compounds **6c**, **6d**, **6f**, **6g**, **6h** and **6i** for K562 cell line was determined as >100 μM. Compound **6j** ranked second among the other compounds for anti-leukemic effects on

K562 cells. The IC_{50} value of compound **6j** was detected 2-fold higher than that of compound **6l** (IC_{50}= 23.84±3.32 μM). The (4-isopropylphenyl)amino moiety also relatively led to increase in anti-leukemia activity. The cytotoxic effects of compounds **6a**, **6k**, **6e** and **6b** on CML cell line were detected 4, 5 and 7-fold less than (IC_{50}= 41.49±9.59 μM, 42.74±7.21 μM, 53.85±10.94 μM, 78.85±12.13 μM, respectively) that of compound **6l** (Table 1).

Comparing our recent results with the previous results [29], it can be concluded that benzyl esters of gypsogenin (compounds **1c**, **GP2** and **GP5**) induced stronger toxicity in K562 cell line (Figure 3) than reductive amination of aldehyde of gypsogenin (compounds **6a-l**).

The cytotoxic effects of compound **6l** and imatinib on different leukemic cells (Jurkat and MT-2) and HeLa cell line were also searched. According to the results as shown in Table 2, compound **6l** demonstrated significant anticancer activity against Jurkat cells (IC_{50}= 12.97± 3.52 μM) compared to imatinib (IC_{50}= 8.15 ± 2.05 μM). However, the cytotoxic effects of compound **6l** on MT-2 and HeLa cells were found weak (IC_{50}= 32.95± 5.92 μM and 49.81± 8.38 μM, respectively). The results manifested that this compound could be effective against T-cell acute lymphoblastic leukemia (T-ALL) (Jurkat cells) along with CML.

It is well-documented that overexpression of Abl TK in hematopoietic cells increases resistance to apoptosis since Abl TK is associated with many downstream signaling pathways that may result in proliferation, suppression of apoptosis, metastasis and angiogenesis in cancer cells [38-41]. Based on its promising cytotoxic activity against K562 cell line, compound **6l** was selected for further studies including determination of its apoptotic effects on K562 cell line and Abl TK inhibitor effects.

For the detection of the apoptotic and necrotic effects of compound **6l** on K562 cell line, CML cell line was subjected to compound **6l** and imatinib at IC_{50} concentrations for 6 h, then stained with Hoechst 33342/annexin V/ethidium homodimer III and observed with a

florescence microscope. This process implies that cells stain with green, yellow and red represent apoptosis, necrosis or late apoptosis, and necrosis respectively. The cells treated with compound **6l** underwent apoptosis mainly in a short time (Fig. 4A). This result suggested that apoptosis was found as the major cell death pathway of compound **6l** (52.4%) when compared with imatinib (61.8%) at an earlier time as shown in Figure 4b. Moreover, compound **6l** revealed 19.1% late apoptosis/necrosis and 28.6% necrosis when compared with imatinib (14.7% and 23.5%, respectively) (Fig. 4B). The difference of apoptosis induction between compound **6l** and imatinib treatment in K562 cells was found not significant (Fig. 4C).

In continuation of searching mechanistic anti-leukemic effects of compound **6l**, its Abl TK inhibitory potential was screened. The results indicated that compound **6l** was able to inhibit Abl TK with an IC_{50} value of 13.04± 2.43 μM. The definite decline for Abl TK inhibition was detected between 0 and 3 μM after imatinib exposure while a similar decline was observed between 10 and 30 μM after compound **6l** implementation as outlined in Fig. 5. Imatinib was used as a standard and showed a stronger inhibitory effect (0.35± 0.21 μM) than compound **6l** on Abl TK. These significant results indicated that compound **6l** showed Abl TK-dependent apoptotic effects.

Apart from Abl TK, the inhibition of compound **6l** was investigated on an extensive group of TK enzymes involving TK-1 (EGFR, HER2, HER4, IGF1R, InsR, KDR, PDGFR-α and PDGFR-β) and TK-2 (BRK, BTK, CSK, FYN A, LCK, LYN B and SRC) in comparison with imatinib at 30 μM concentration. In TK-1 panel, the difference between inhibitory effects of compound **6l** and imatinib on IGF1R, InsR and KDR was observed not significant, whereas it was observed significant on EGFR, HER-2, PDGFR-α and PDGFR-β inhibition. In TK-2 panel, this difference was found significant for BRK, CSK, FYN A, LCK and LYN B inhibition and not significant for BTK and SRC inhibition (Fig. 6). In TK-1 panel, it was

determined that compound **6l** was also capable of inhibiting epidermal growth factor receptor (EGFR) (60%) significantly followed by HER2, HER4 and KDR (39%, 19% and 18%, respectively) (Fig. 6). EGFR (HER-1/ERBB1) belongs to ERBB family of receptor tyrosine kinases along with three other closely related receptors, namely HER-2 (ERBB2), HER-3 (ERBB3) and HER-4 (ERBB4). Abundant evidence showed that EGFR was also mutated and/or overexpressed in different types of cancer such as non-small cell lung cancer (NSCLC), glioblastoma, colorectal cancer and pancreatic cancer [42, 43]. Correspondingly, compound **6l** could be investigated for future EGFR-focused anticancer studies.

In TK-1 system, imatinib also possessed a more distinct inhibitory profile than compound **6l** showing remarkable inhibitory effects on PDGFR-α and PDGFR-β, which were reported to be dysregulated with high rates in a number of cancer types such as melanoma, lung cancer and glioblastoma [44].

Compound **6l** showed no significant inhibition except for Abl TK in TK-2 profiling system indicating its selective Abl TK inhibitory potency. At this point, imatinib served a very different inhibitory profile than compound **6l** inhibiting LCK and LYN B notably.

Overall, it is obvious that compound **6l** exhibited the most promising inhibitory effects towards Abl TK among all tested TK-1 and TK-2 members indicating its selective mode of action.

2.4. In silico evaluation

Based on potential *in vitro* Abl TK inhibitor effects of compound **6l**, molecular docking studies were conducted to elucidate the feasible binding modes of compound **6l** *via* Maestro software (Schrödinger Release 2016-2: Schrödinger, LLC, New York, USA) in the ATP-binding pocket of Abl TK (PDB code: 2HYY) [45] compared with the standard agent imatinib and compounds **6a-k** (Fig 7A and 7B). Results revealed that compound **6l** presented high affinity forming favorable interactions similar with imatinib (Asp381 and His361) (Fig.

8A and 8B). In particular, the amine part of compound **6l** formed crucial salt-bridge formation and π-cation with Asp381 and His361, respectively at ionization state just same as in the 4-(methylpiperazin-1-yl) moiety of imatinib (Fig. 9). This outcome also highlighted that 4-(methylphenyl)amino moiety was crucial for binding profile of compound **6l** to the ATP-binding pocket of Abl kinase supporting the *in vitro* findings. Moreover, compound **6l** displayed hydrogen bonding and salt-bridge formation with Lys285 by virtue of its carboxylic acid part. Compound **6l** missed the key interactions of imatinib with Met318 and Tyr253 interpreting its less significant Abl inhibitory profile compared to imatinib. For the purpose of comparing the different conformations of the same ligand, the emodel score is generally preferred, while the different ligands are compared using the docking score [46]. All docking scores of the compounds were determined to range from -3.564 kcal/mol to -6.021 kcal/mol (Table 2). In general, the docking scores of compounds were consistent with the biological data. The docking scores with the lowest energy (high negative scores), belonging to compound **6l** explained its high inhibitory potency and binding capacity to the ATP-binding cleft of Abl TK. Compound **6j** ranked second also for the docking score with -5.927 kcal/mol but this compound formed no interaction in the ATP binding cleft of Abl TK (Fig. 9).

Some crucial ADME (Absorption, Distribution, Metabolism and Excretion) parameters of compound **6l** such as brain/blood partition coefficient (QPlogBB), central nervous system (CNS) activity, human oral absorption and in concordance with Lipinski's rule of 5 and Jorgensen's rule of 3 were *in silico* predicted in order to postulate the drug similarities of compounds **6a-l**. The outcomes depicted in Table 4 were found in admissible range linked with the specified parameters for compound **6l**. The QPlogBB and CNS values of compound **6l** were detected as -0.773 and -1, respectively. Compound **6l** was determined to exhibit excellent absorption (91.265%) on a 0-100% scale (>80% is high; <25% is poor).

Furthermore, compound **6l** revealed violation for two parameters of Lipinski's rule of 5 (maximum is four) and one parameter of Jorgensen's rule of 3 (maximum is three). The QPlogBB and CNS values of compounds **6a-k** were found in the range of -1.857 to 0.096 and -2 to 0, respectively. Compounds **6a-k** revealed distinct absorption values as 53.760 to 94.757 on a 0-100% scale. Compounds **6a-k** violated one or two parameters of Lipinski's rule of 5 and Jorgensen's rule of 3.

3. Conclusion

In the current study, we aimed to design and synthesize new semi-synthetic gypsogenin derivatives and further investigate their mechanistic effects on CML. We synthesized twelve new gypsogenin derivatives *via* well-established and facile methods. These derivatives were evaluated against initially K562 CML cell line and PBMCs (healthy). Compound **6l** revealed the highest and selective cytotoxicity against CML cells compared to imatinib. The IC_{50} value was found as 14.32 ± 2.04 μM for compound **6l** against CML cells compared to imatinib (IC_{50}= 4.89 ± 1.86 μM). Following CML cells, this derivative was also found to be effective against Jurkat cells with an IC_{50} value of 12.97± 3.52 μM. Further mechanistic experiments showed that compound **6l** was apoptotic in CML cells and inhibited Abl TK significantly among a large panel of kinases compared to imatinib indicating Abl TK-dependent apoptotic potential of this compound in CML cells. Molecular docking studies also supported these *in vitro* findings revealing key interactions of compound **6l** in the ATP-binding cleft of Abl TK. Besides, *in silico* ADME results of compound **6l** were in agreement with the specified limits that makes this compound a proper drug candidate for future CML-focused anticancer studies.

4. Experimental

4.1. Chemistry

For all compounds, melting points (m.p.) were detected with a Gallen-kamp

electrothermal melting point apparatus (uncorrected ±0.1 °C). IR spectra were measured on a Perkin-Elmer Frontier FT/IR spectrometer. LC-MS was recorded on an Thermo Scientific/ Surveyor MSQ spectrometer. ^{1}H NMR spectra (600 MHz) and ^{13}C NMR (150 MHz) spectra were recorded on Agilent spectrometer. Column chromatography was performed using 60 Å silica gel (Merck 7734). Thin-layer chromatography (TLC) was performed using 60 Å silica gel on F254 aluminum plates (Merck 5554).

*4.1.1. General method for the preparation of gypsogenin (**1**)*

After the commercially available water extract of *Gypsophila arrostii* roots, gypsogenin (*3-Hydroxy-23-oxoolean-12-en-28-oic acid)* (**1**) was prepared according to a literature procedure [22].

*4.1.2. 3-Hydroxy-23-oxoolean-12-en-28-oic acid gypsogenin (**1**))*

m.p.: 273-274 ^{0}C; LC/MS (ESI-MS) m/z = 469.20 [M-1] (negative ion mode)

*4.1.3. General procedure for the synthesis of compounds (**6a-l**)*

Semi-synthesis is the process of using an available natural analogue as a starting material to achieve new compounds with reasonable amounts and desirable chemical and medicinal properties. This method is more efficient and cheaper compared to total synthesis since fewer chemical steps are required usually combined with extraction protocols for catalytic conversions [35-47].

Amine derivatives (R. **a-l**) (0.46 mmol) were added to a solution of gypsogenin (**1**) (200 mg, 0.420 mmol) in dichloroethane (3 mL). Then, $NaBH(OAc)_3$ (126 mg, 0.59 mmol) was added and the mixture was stirred for 24h at room temperature under an N_2 atmosphere. Afterwards, the mixture was added to water and extracted with AcOEt. The obtained organic layer was dried over anhydrous Na_2SO_4 and concentrated in vacuo. The residue was purified with different silica gel chromatography (hexane/ethyl acetate (1/1) or dichlorometane/ethyl acetate (1/1)) to afford compounds **6a-l** [30, 31].

4.1.3.1. (3β)-3-Hydroxy-23-(4-methyl-1H-pyrazol-1-yl)olean-12-en-28-oic acid ***(6a)***

Rf = 0.40 (DCM/AcOEt 1:1); White solid; Yield: 51 %; m.p. 132.5-133.3 °C ; FT-IR KBr (cm^{-1}): 3443, 2924, 2848, 1742, 1642, 1456, 1380, 1262, 1027, 749; ^{1}H-NMR (600 MHz, DMSO-d_6): δ= 0.68 (H-24), 0.89 (H-26), 0.90 (H-29), 0.93 (H-25), 0.97 (H-30), 1.15 (H-27), 1.98 (s, 3H, -C<u>H</u>x$_3$), 3.03 (dd, H-18), 4.11 (H-3), 4.35 (H-23), 5.14 (br s, H-12), 5.72 (H-5a), 7.33 (1H, H-3a); APT-NMR (150 MHz, DMSO-d_6): δ= 7.2 (CHx3), 11.3 (C-24), 14.8 (C-25), 16.3 (C-26), 22.5 (C-30), 25.0 (C-27), 30.3 (C-20), 32.0 (C-7), 32.1 (C-29), 33.4 (C-21), 38.1 (C-10), 39.1 (C-4), 41.5 (C-18), 42.8 (C-19), 45.8 (C-8), 49.3 (C-5), 65.7 (C-4), 72.4 (C-3), 116.3 (C-4a), 122.4 (C-12), 132.4 (C-5a), 137.4 (C-3a), 143.8 (C-13), 196.0 (C-28); LC/MS (ESI-MS) *m/z* Calc for $C_{34}H_{52}N_2O_3$ 536.62 $[M]^-$ Found: 536.64

4.1.3.2. (3β)-3-Hydroxy-23-(4-methylpiperazin-1-yl)olean-12-en-28-oic acid ***(6b)***

Rf: 0.38 (DCM/AcOEt 1:1); White solid; Yield: 44%; m.p. 122.1-124.5 °C ; FT-IR KBr (cm^{-1}): 3446, 2924, 2853, 1737, 1634, 1460, 1384, 1376, 1265, 1186, 1007, 743; ^{1}H-NMR (600 MHz, DMSO-d_6): δ= 0.48 (s, H-24), 0.63 (s, H-25), 0.79 (s, H-26), 0.81 (s, H-30), 0.85 (s, H-29), 1.02 (s, H-27), 2.14 (s, 3H, -NC<u>H</u>$_3$), 2.23-2.33 (m, 4H, H-3a/5a), 2.43-2.38 (m, 4H, H-2a/6a), 2.46 (dd, J= 7.2, 13.8 Hz, H-18), 3.29 (s, H-23), 3.41 (m, H-3), 5.06 (brs, H-12); APT-NMR (150 MHz, DMSO-d_6): δ= 12.9 (C-24), 15.8 (C-29), 16.9 (C-25), 17.8 (C-6), 23.3 (C-26), 23.8 (C-11), 25.8 (C-27), 27.6 (C-15), 32.1 (C-20), 32.6 (C-7), 33.0 (C-30), 33.8 (C-22), 36.6 (C-21), 38.3 (C-1), 39.0 (C-18), 40.8 (C-4), 45.5 (-NCH_3), 51.7 (C-2a/6a), 54.6 (C-3a/5a), 55.1 (C-5), 64.8 (C-23), 70.9 (C-3), 121.7 (C-12), 144.5 (C-13), 179.9 (C-28); LC/MS (ESI-MS) *m/z* Calc for $C_{35}H_{58}N_2O_2$ 555.70 $[M]^-$ Found: 555.72

4.1.3.3. (3β)-23-[(1-Benzylpiperidin-4-yl)imino]-3-hydroxyolean-12-en-28-oic acid ***(6c)***

Rf: 0.44 (DCM/AcOEt 1:1); White solid; Yield: 39%; m.p. 240.1-243.4 °C ; FT-IR KBr (cm^{-1}): 3449, 2925, 2854, 1731, 1462, 1383, 1274, 1124, 1072, 748; ^{1}H-NMR (600 MHz, Methanol-d_6): δ= 0.68 (H-25), 0.81 (H-30), 0.90 (H-29), 0.91 (H-26), 0.94 (H-27), 0.92

(H-24), 1.40 (m, H-2a/6a), 2.81 (m, H-3a/5a), 3.26 (H-1a), 3.28 (H-23), 3.66 (H-3), 3.26 (H-1a), 3.40 (H-18), 4.19 (-CH_X2), 5.14 (br s, H-12), 7.60 (m, H-3b/5b), 7.71 (H-2b/6b); APT-NMR (150 MHz, Methanol-d_6): δ= 9.8 (C-24), 11.1 (C-25), 12.8 (C-26), 16.2 (C-30), 22.4 (C-27), 28.8 (C-2a/6a), 31.8 (C-20), 32.1 (C-29), 32.5 (C-7), 33.6 (C-22), 36.4 (C-10), 37.8 (C-1), 39.2 (C-4), 41.1 (C-18), 48.9 (C-19), 65.8 (C-23), 65.9 (C-1a), 67.6 (Cx), 72.4 (C-3), 122.3 (C-12), 124.2 (C-4b), 128.5 (C-3b/5b), 130.9 (C-2b/6b), 132.2 (C-1b), 143.8 (C-13), 178.3 (C-28); LC/MS (ESI-MS) *m/z* Calc for $C_{42}H_{64}N_2O_3$ 647.27 $[M+2]^+$ Found: 647.29

*4.1.3.4. (3β)-3-Hydroxy-23-(4-pyrimidin-2-ylpiperazin-1-yl)olean-12-en-28-oic acid (**6d**)*

Rf: 0.40 (DCM/AcOEt 1:1); White solid; Yield: 62%; m.p. 253.8-255.3 °C ; FT-IR KBr (cm^{-1}): 3444, 2923, 2853, 1634, 1452, 1384, 1275, 1264, 1032, 745; ^{1}H-NMR (600 MHz, DMSO-d_6): δ= 0.50 (H-24), 0.67 (H-26), 0.83 (H-29), 0.84 (H-30), 0.84 (H-25), 1.05 (H-27), 2.11-2.50 (H-2a/6a), 2.71 (H-23), 3.04 (d, H-18), 3.29 (d, H-3), 4.17-4.40 (H-3a/5a), 5.13 (br s, H-12), 6.58 (H-4b), 8.33 (1H, H-3b/5b); APT-NMR (150 MHz, DMSO-d_6): δ= 12.9 (C-24), 15.7 (C-25), 16.9 (C-26), 18.02 (C-6), 23.0 (C-11), 23.3 (C-16), 23.6 (C-30), 25.9 (C-27), 30.9 (C-15), 33.0 (C-29), 36.7 (C-20), 38.3 (C-3a/5a), 40.9 (C-18), 41.6 (C-4), 45.9 (C-2a/6a), 59.9 (C-5), 64.5 (C-23), 70.3 (C-3), 110.5 (C-4b), 121.8 (C-12), 144.3 (C-13), 158.4 (C-3b/5b), 161.4 (C-1b), 181.2 (C-28). ESI-MS m/z Calc for $C_{38}H_{58}N_4O_3$ 517.86 $[M-(C_4H_3N_2)-Na+1]^+$, Found: 517.87

*4.1.3.5. (3β)-23-(4,5-Dihydro-1,3-thiazol-2-ylamino)-3-hydroxyolean-12-en-28-oic acid (**6e**)*

Rf: 0.40 (DCM/AcOEt 1:1); White solid; Yield: 67%; m.p. 117.4-188.5 °C ; FT-IR KBr (cm^{-1}): 3444, 2924, 2853, 2065, 1634, 1461, 1275, 1262, 749; ^{1}H-NMR (600 MHz, DMSO-d_6): δ= 0.48 (H-24), 0.69 (H-26), 0.83 (H-30), 0.84 (H-25), 1.05 (H-27), 1.85 (H-29), 2.70 (dd, H-18), 3.05- 3.26 (H-23), 3.31 (-C$\underline{H}_2$S), 3.42 (H-3), 4.06 (-C$\underline{H}_2$N), 5.13 (br s, H-12); APT-NMR (150 MHz, DMSO-d_6): δ= 12.8 (C-24), 15.8 (C-25), 17.2 (C-26), 17.9 (C-6), 23.1 (C-11), 23.4 (C-16), 23.9 (C-30), 25.9 (C-27), 30.9 (C-15), 33.0 (C-29), 33.7 (C-20),

36.7 (C-7), 38.3 (C-22), 40.7 (C-18), 60.5 (C-23), 64.5 (CH$_2$-S), 67.6 (CH$_2$-N), 70.4 (C-3), 121.8 (C-12), 144.5 (C-13), 167.4 (C-NH), 178,9 (C-28); LC/MS (ESI-MS) *m/z* Calc for ($C_{33}H_{52}N_2O_3S$) 553.29 $[M+2]^+$ Found: 553.30

*4.1.3.6. (3β)-23-[(4-Chloro-2-sulfophenyl)amino]-3-hydroxyolean-12-en-28-oic acid (**6f**)*

Rf: 0.40 (DCM/AcOEt 1:1); White solid; Yield: 51 %; m.p. 132.5-133.9 °C ; FT-IR KBr (cm^{-1}): 3444, 2924, 2848, 1742, 1642, 1456, 1380, 1262, 1027, 749; ^{1}H-NMR (600 MHz, DMSO-d_6): δ= 0.48 (H-24), 0.69 (H-24), 0.89 (H-25), 0.89 (H-26), 0.93 (H-29), 0.97 (H-30), 1.16 (H-27), 2.70 (dd, H-18), 3.05 (H-3), 3.28 (H-23), 5.13 (br s, H-12), 7.26 (1H, H-6a), 7.66 (1H, H-5a), 8.07 (1H, H-3a); APT-NMR (150 MHz, DMSO-d_6): δ= 9.9 (C-24), 11.2 (C-25), 12.9 (C-26), 13.5 (C-6), 14.8 (C-30), 15.3 (C-2), 16.3 (C-27), 17.7 (C-15), 22.5 (C-29), 30.2 (C-20), 32.1 (C-7), 32.4 (C-22), 33.6 (C-21), 36.6 (C-10), 38.0 (C-8), 39.1 (C-4), 40.9 (C-18), 42.0 (C-14), 51.2 (C-23), 67.7 (C-4), 72.4 (C-3), 122.1 (C-6a), 122.2 (C-12), 126.4 (C-4a), 128.4 (C-5a), 131.1 (C-3a), 132.2 (C-2a), 143.8 (C-13), 144.6 (C-1a); LC/MS (ESI-MS) *m/z* Calc for $C_{36}H_{52}ClNO_6S$ 663.39 $[M+1]^+$ Found: 663.40

*4.1.3.7. (3β)-23-[(3-Cyanophenyl)amino]-3-hydroxyolean-12-en-28-oic acid (**6g**)*

Rf: 0.42 (DCM/AcOEt 1:1); White solid; Yield: 44 %; m.p. 122.1-124.5 °C ; FT-IR KBr (cm^{-1}): 3446, 2924, 2853, 1737, 1694, 1460, 1384, 1376, 1265, 1186, 1007, 743; ^{1}H-NMR (600 MHz, DMSO-d_6): δ= 0.50 (H-24), 0.67 (H-26), 0.83 (H-29), 0.84 (H-25), 0.85 (H-30), 1.05 (H-27), 2.71 (dd, H-18), 3.01-3.27 (H-23), 3.37 (H-3), 5.14 (br s, H-12), 7.66 (1H, H-2a), 7.69 (1H, H-6a), 8.07 (H-4a/5a); APT-NMR (150 MHz, DMSO-d_6): δ= 12.8 (C-24), 15.6 (C-25), 17.0 (C-26), 17.9 (C-6), 19.3 (C-11), 22.8 (C-16), 23.5 (C-30), 25.1 (C-2), 25.8 (C-27), 30.5 (C-15), 33.0 (C-29), 33.7 (C-20), 38.3 (C-22), 39.3 (C-21), 41.0 (C-18), 64.5 (C-23), 70.4 (C-3), 111.7 (C-3a), 129.1 (C-6a), 121.8 (C-12), 132.0 (C-2a), 130.7 (C-5a), 129.8 (C-4a), 144.0 (C-13), 167.4 (C-1a), 179.1 (C-28); LC/MS (ESI-MS) *m/z* Calc for $C_{37}H_{52}N_2O_3$ 572.80 $[M+K+1]^+$ Found: 572.82

*4.1.3.8. (3β)-3-Hydroxy-23-{[4-(trifluoromethyl)pyridin-2-yl]amino}olean-12-en-28-oic acid (**6h**)*

Rf: 0.40 (DCM/AcOEt 1:1); White solid; Yield: 58%; m.p. 126.6-127.3 °C ; FT-IR KBr (cm^{-1}): 3445, 2923, 2853, 1634, 1461, 1275, 1262, 749; ^{1}H-NMR (600 MHz, DMSO-d_6): δ= 0.50 (H-24), 0.68 (H-26), 0.83 (H-27), 0.85 (H-25), 1.05 (H-30), 1.08 (H-29), 2.72 (dd, H-18), 3.29 (d, H-3), 3.05-3.30 (H-23), 5.13 (br s, H-12), 6.50 (1H, -NH), 6.72 (1H, H-6a), 7.60 (1H, H-4a), 8.18 (1H, H-3a); APT-NMR (150 MHz, DMSO-d_6): δ= 11.5 (C-24), 12.8 (C-25), 17.1 (C-30), 17.9 (C-6), 22.9 (C-11), 23.4 (C-16), 23.6 (C-27), 24.8 (C-2), 25.7 (C-26), 25.9 (C-29), 40.9 (C-18), 64.7 (C-4), 64.7 (C-23), 78.3 (C-3), 107.9 (C-6a), 121.6 (-$\underline{C}F_3$), 122.1 (C-12), 134.4 (C-5a), 144.0 (C-13), 146.1 (C-3a), 178.9 (C-28); LC/MS (ESI-MS) *m/z* Calc for $C_{36}H_{51}F_3N_2O_3$ 617.15 $[M+1]^+$ Found: 617.17

*4.1.3.9. (3β)-3-Hydroxy-23-[(4-methoxyphenyl)amino] olean-12-en-28-oic acid (**6i**)*

Rf: 0.46 (DCM/AcOEt 1:1); White solid; Yield: 78 %; m.p. 248-250 °C ; FT-IR KBr (cm^{-1}): 3456, 2924, 2853, 1637, 1461, 1384, 1262, 748; ^{1}H-NMR (600 MHz, DMSO-d_6): δ= 0.55 (H-24), 0.69 (s, H-26), 0.84 (s, H-30), 0.85 (s, H-25), 0.86 (s, H-29), 1.06 (s, H-27), 2.72 (dd, H-18), 3.06-3.31 (s, H-23), 3.42 (m, H-3), 3.67 (s, 3H, -OCH_3), 5.12 (brs, H-12), 5.74 (bs, 1H, -NH), 6.83 (2H, d, J=7.6 Hz, H-3a/5a), 7.46 (2H, d, J=7.6 Hz, H-2a/6a); APT-NMR (150 MHz, DMSO-d_6): δ= 13.1 (C-24), 15.6 (C-25), 23.8 (C-26), 17.9 (C-6), 23.1 (C-11), 23.3 (C-11), 24.1 (C-27), 25.9 (C-30), 30.9 (C-20), 32.5 (C-7), 33.1 (C-29), 33.7 (C-22), 36.6 (C-21), 39.2 (C-8), 40.4 (C-4), 41.3 (C-18), 42.6 (C-14), 45.8 (C-19), 55.5 (-O$\underline{C}H_3$), 64.6 (C-23), 70.5 (C-3), 114.2 (C-3a/5a), 120.9 (C-2a/6a), 120.9 (C-12), 132.9 (C-1a), 155.4 (C-6a), 178.5 (C-28); LC/MS (ESI-MS) *m/z* Calc for $C_{37}H_{55}NO_4$ 578,33 $[M+1]^+$ Found: 577.35

*4.1.3.10. (3β)-3-Hydroxy-23-[(4-isopropylphenyl)amino] olean-12-en-28-oic acid (**6j**)*

Rf: 0.45 (Hexane/AcOEt 1:1); White solid; Yield: 32 %; m.p. 153.3-154.6 °C ; FT-IR KBr (cm^{-1}): 3453, 2924, 2857, 1636, 1462, 1376, 1281, 1033, 750; ^{1}H-NMR (600 MHz,

DMSO-d_6): δ= 0.51 (H-24), 0.69 (s, H-26), 0.83 (s, H-29), 0.83 (s, H-30), 0.85 (s, H-25), 1.07 (s, H-27), 1.15 (d, C<u>H</u>$_3$), 2.72 (dd, H-18), 2.82 (m, C<u>H</u>- CH_3), 3.06-3.32 (H-23), 3.40 (d, H-3), 5.14 (br s, H-12), 7.11 (d, H-2a/6a), 7.45 (d, H-3a/5a); APT-NMR (150 MHz, DMSO-d_6): δ= 12.8 (C-24), 15.8 (C-25), 17.3 (C-26), 17.9 (C-6), 23.2 (C-16), 23.8 (C-30), 23.9 (-**<u>C</u>**H_3-CH), 26.1 (C-27), 26.9 (C-2), 27.6 (C-15), 30.8 (C-20), 32.6 (C-7), 32.9 (-**<u>C</u>**H-CH_3), 33.0 (C-29), 33.8 (C-22), 34.9 (C-21), 36.7 (C-1a), 38.2 (C-1), 41.0 (C-18), 41.6 (C-4), 42.3 (C-14), 64.7 (C-23), 70.6 (C-3), 119.5 (C-3a/5a), 121.8 (C-12), 126.8 (C-2a/6a), 143.4 (C-13), 179.0 (C-28); LC/MS (ESI-MS) *m/z* Calc for $C_{39}H_{59}NO_3$ 590.26 $[M+1]^+$, Found: 590.28

*4.1.3.11. (3β)-3-Hydroxy-23-[(4-nitrophenyl)amino]olean-12-en-28-oic acid (**6k**)*

Rf: 0.46 (Hexane/AcOEt 1:1); White solid; Yield: 64 %; m.p. 197.4-199.1 °C ; FT-IR KBr (cm^{-1}): 3453, 2924, 2854, 1732, 1641, 1462,1380,1260, 749; ^{1}H-NMR (600 MHz, DMSO-d_6): δ= 0.69 (H-24), 0.80 (H-25), 0.85 (H-26), 0.89 (H-30), 1.07 (H-29), 1.20 (H-27), 2.70 (dd, J= 6.8, 13.6 Hz, H-18), 3.59 (m, H-3), 5.14 (brs, H-12), 7.10 (-N<u>H</u>), 7.30 (d, H-2a/6a), 7.80 (d, H-3a/5a); APT-NMR (150 MHz, DMSO-d_6): δ= 11.7 (C-24), 16.1 (C-25), 17.2 (C-26), 18.3 (C-6), 23.2 (C-11), 23.8 (C-30), 24.7 (C-16), 26.1 (C-27), 27.6 (C-2), 28.7 (C-15), 30.8 (C-20), 32.3 (C-7), 33.2 (C-29), 33.6 (C-22), 37.0 (C-10), 37.8 (C-1), 38.0 (C-8), 41.2 (C-18), 41.7 (C-4), 45.8 (C-14), 46.1 (C-19), 47.2 (C-9), 51.5 (C-5), 78.1 (C-3), 120.4 (C-2a/6a), 121.6 (C-12), 125.0 (C-3a/5a), 138.1 (C-4a), 144.3 (C-13), 159.0 (C-1a), 179.1 (C-28); LC/MS (ESI-MS) *m/z* Calc for $C_{36}H_{52}N_2O_5$ 616.89 $[M+Na+1]^+$ Found: 616.90

*4.1.3.12. (3β)-3-Hydroxy-23-[(4-methylphenyl)amino] olean-12-en-28-oic acid (**6l**)*

Rf: 0.32 (Hexane/AcOEt 1:1); White solid; Yield: 25 %; m.p. 215.6-216.3 °C ; FT-IR KBr (cm^{-1}): 3444, 2927, 2842, 2075, 1633, 1459, 1053, 1033, 1015, 763; ^{1}H-NMR (600 MHz, DMSO-d_6): δ= 0.51 (H-24), 0.69 (H-25), 0.85 (H-26), 0.89 (H-30), 1.08 (H-29), 1.10 (H-27), 2.01 (-C<u>H</u>x$_3$), 2.72 (dd, H-18), 3.03-3.14 (m, H-23), 3.30 (m, H-3), 5.14 (brs, H-12), 7.06 (d, J= 7.8 Hz, H-2a/6a), 7.42 (d, J= 7.8 Hz, H-3a/5a); APT-NMR (150 MHz, DMSO-d_6):

δ= 13.1 (C-24), 15.9 (C-25),17.3 (C-26), 17.9 (C-6), 20.8 (CH_x3), 23.0 (C-11), 23.3 (C-16), 23.8 (C-30), 26.0 (C-27), 26.9 (C-2), 27.6 (C-15), 30.7 (C-20), 32.3 (C-7), 32.5 (C-22), 33.3 (C-29), 33.7 (C-21), 36.7 (C-10), 38.3 (C-1), 39.2 (C-8), 40.3 (C-4), 41.2 (C-18), 41.7 (C-14), 45.9 (C-19), 46.0 (C-17), 46.8 (C-9), 47.5 (C-5), 64.3 (C-23), 70.6 (C-3), 119.5 (C2a/C-6a), 122.0 (C-12), 129.6 (C-3a/C-5a), 132.1 (C-4a), 137.2 (C-1a), 144.1 (C-13), 179.0 (C-28); LC/MS (ESI-MS) *m/z* Calc for $C_{37}H_{55}NO_3$ 544,75 $[(M-H_2O)+1]^+$ Found: 544.73

4.2. Biological activity

4.2.1. In vitro cytotoxicity

K562, Jurkat, MT-2 and healthy (Precision Bioservices, Frederic, MD) cells were cultured in RPMI 1640 (Wako Pure Chemical Industries), while HeLa cells were cultured in DMEM (Wako Pure Chemical Industries). All cells were enriched with 10% fetal bovine serum (FBS) (Sigma Aldrich, MO, USA) and 85 µg/mL streptomycin (Meiji Seika Pharma, Tokyo, Japan) at proper conditions. These cancer cells and PBMCs were cultured in 24-well (4×10^4 cells/mL conc.) and 96-well (1×10^6 cells/mL conc.) plates (Iwaki brand Asahi Glass Co., Chiba, Japan), respectively for 48 h. The stock solution of gypsogenin derivatives and imatinib were prepared in DMSO (Wako Pure Chemical Industries) (conc. between 0.1-10 mM) and further diluted with fresh culture medium. The DMSO concentration in the last culture medium was 1% showing no effect on the cell viability [29].

The effect of gypsogenin derivatives and imatinib on cell viability was screened by MTT (Dojindo Molecular Technologies, Kumamoto, Japan) as previously mentioned in the literature [29] and all experiments were repeated in triplicate.

4.2.2. Detection of apoptosis

K562 cells (4×10^4 cells/well) were incubated in each well of 24-well plate with the most effective gypsogenin derivative in this series at IC_{50} concentrations for 6 h. Then, apoptosis detection kit from PromoKine, Heidelberg, Germany was performed according to

guidance of manufacturer as previously explained [48].

4.2.3. TK inhibitory activity

TK profiling assay protocol (TK1 and TK-2) was carried out based on the manufacturer`s instructions (Promega Corporation, Madison, WI, USA) with little modifications [28, 29] and the IC_{50} values of tested compounds required to decrease the TK activity by 50% were calculated by ImageJ software.

4.2.4. Statistical analysis

All results were demonstrated as means ± SD. Data were analyzed using one-way analysis of variance and differences were considered significant at $^{*}p < 0.05$, $^{**}p < 0.005$, $^{\#}p < 0.0005$, $^{\#\#}p < 0.0001$. The IC_{50} were detected by statistical software, GraphPad Prism7 (GraphPad Software, San Diego, CA, USA) [49, 50]

4.3. In silico evaluation

4.3.1. Molecular docking studies

The crystal structure of the Abl TK with imatinib was acquired from the RSCB database (PDB ID: 2HYY) [45]. The raw file was prepared for the docking assessment by the PrepWizard module of Maestro. The missing chains were added automatically by Prime and the protonation state was calculated by PropKa at physiological pH. Grid generation of Maestro was used to determine the docking grid, which was centered on the crystallographic inhibitor present in the crystal structure and extended to a space of 25 × 25 × 25 Angstrom. The generated grid was used for the further docking experiments. Compounds **6a-l** were sketched and cleaned in Maestro workspace and were prepared with energy minimization using OPLS_2005 force field at physiological pH using the LigPrep module. The obtained ligands were submitted to Glide/XP docking protocols [51].

4.3.2. ADME studies

Some crucial pharmacokinetic features of compounds **6a-l** were estimated by QikProp

(QikProp, Schrödinger, LLC, New York, 2016). Ligands were prepared in the LigPrep module of Maestro. The obtained ligands were applied to Ligand-based ADME/Tox Prediction for computation of some defined determinants [51-53].

Acknowledgements

This study was supported by 2544 Scientific and Technological Research Institution of Turkey (TUBITAK) and Japan Society for the Promotion of Science (JSPS) Bilateral Cooperation Project (No.117R034). This publication has been produced benefiting from TUBITAK 2236 CoCirculation2, grant number 121C063. However, the entire responsibility of the publication belongs to the authors. The financial support received from TUBITAK does not mean that the content of the publication is approved in a scientific sense by TUBITAK.

References

[1] M. Breccia, G. Alimena, Activity and safety of dasatinib as second-line treatment or in newly diagnosed chronic phase chronic myeloid leukemia patients, BioDrugs. 25 (2011) 147-157.

[2] M. Bonifacio, F. Stagno, L. Scaffidi, M. Krampera, F. Di Raimondo, Management of chronic myeloid leukemia in advanced phase, Front. Oncol. 9 (2019) 1132.

[3] E. Zanforlin, G. Zagotto, G. Ribaudo, A chemical approach to overcome tyrosine kinase inhibitors resistance: Learning from chronic myeloid leukemia, Curr. Med. Chem. 26 (2019) 6033-6052.

[4] F. Carofiglio, D. Trisciuzzi, N. Gambacorta, F. Leonetti, A. Stefanachi, O. Nicolotti, Bcr-Abl allosteric inhibitors: Where we are and where we are going to, Molecules. 25 (2020) 4210.

[5] V.K. Singh, M.S. Coumar, Chronic myeloid leukemia: existing therapeutic options and strategies to overcome drug resistance, Mini Rev. Med. Chem. 19 (2019) 333-345.

[6] C. Walz, M. Sattler, Novel targeted therapies to overcome imatinib mesylate resistance in chronic myeloid leukemia (CML), Crit. Rev. Oncol. Hematol. 57 (2006) 145-164.

[7] M. Breccia, G. Alimena, The current role of high-dose imatinib in chronic myeloid leukemia patients, newly diagnosed or resistant to standard dose, Expert Opin. Pharmacother. 12 (2011) 2075-2087.

[8] N. Shibata, N. Ohoka, T. Hattori, M. Naito, Development of a potent protein degrader against oncogenic BCR-ABL protein, Chem. Pharm. Bull. (Tokyo). 67 (2019) 165-172.

[9] N. Javidi-Sharifi, G. Hobbs, Future Directions in Chronic Phase CML Treatment, Curr. Hematol. Malig. Rep. 16 (2021) 500-508.

[10] E. Jabbour, H. Kantarjian, Chronic myeloid leukemia: 2020 update on diagnosis, therapy and monitoring, Am. J. Hematol. 95 (2020) 691-709

[11] P.E. Westerweel, P.A.W. Te Boekhorst, M.C. Levin, J.J. Cornelissen, New approaches and treatment combinations for the management of chronic myeloid leukemia, Front. Oncol. 9 (2019) 665.

[12] B. Yin, D.M. Fang, X.L. Zhou, F. Gao, Natural products as important tyrosine kinase inhibitors, Eur. J. Med. Chem. 182 (2019) 111664.

[13] P. Parcha, S. Sarvagalla, B. Madhuri, S. Pajaniradje, V. Baskaran, M.S. Coumar, B. Rajasekaran, Identification of natural inhibitors of Bcr-Abl for the treatment of chronic myeloid leukemia, Chem. Biol. Drug Des. 90 (2017) 596-608.

[14] J.-R. Wang, H. Zhou, Z.-H. Jiang, L. Liu, Two new triterpene saponins from the anti-inflammatory saponin fraction of Ilex pubescens root, Chem. Biodivers. 5 (2008) 1369-1376.

[15] I.N. Karasteva, R.A. Toshkova, S.D. Nikolov, Protective effect of Astragalus corniculatus saponins against myeloid graffi tumour in hamsters, Phytotherapy Res. 18 (2004) 255-257.

[16] S.-C. Bang, J.-H. Lee, G.-Y. Song, D.-H. Kim, M.-Y. Yoon, B.-Z. Ahn, Antitumor

activity of Pulsatilla koreana saponins and their structure-activity relationship, Chem. Pharm. Bull. 53 (2005) 1451-1454.

[17] K. Hostettmann, A. Marston, Chemistry and pharmacology of natural products: Saponins, Cambridge University Press, 1995.

[18] D. Frechet, B. Christ, B.M. Sorbier, H. Fischer, M. Vuilhorgne, Four triterpenoid saponins from dried roots of Gypsophila species, Phytochemistry. 30 (1991) 927-931.

[19] Q. Chen, J.-G. Luo, L.-Y. Kong, New triterpenoid saponins from the roots of Gypsophila perfoliata Linn, Carbohydr. Res. 346 (2011) 2206-2212.

[20] M. Henry, M. Rochd, B. Bennini, Phytochemistry, 30 (2005) 1819-1821.

[21] S. Emirdag-Ozturk, T. Karayildirim, A. Capaci-Karagoz, O. Alankus-Caliskan, A. Ozmen, E. Poyrazoglu-Coban, Synthesis, antimicrobial and cytotoxic activities, and structure-activity relationships of gypsogenin derivatives against human cancer cells, Eur. J. Med. Chem. 82 (2014) 565-573.

[22] S.E. Ozturk, I. Babahan, A. Ozmen, Synthesis, characterization and *in vitro* anti-neoplastic activity of gypsogenin derivatives, Bioorg. Chem. 53 (2014) 15-23.

[23] Y. Lu, D. Van, L. Deibert, G. Bishop, J. Balsevich, Phytochemistry Antiproliferative quillaic acid and gypsogenin saponins from *Saponaria officinalis* L. roots, Phytochemistry. 113 (2015) 108-120.

[24] Y. Liu, X. Li, S. Jiang, Q. Ge, Inhibitory effect of Gypsophila oldhamiana gypsogenin on NCI-N87 gastric cancer cell line, Eur. J. Inflamm. 16 (2018) 1-11.

[25] G. Wu, H. Chu, J. Wang, Y. Mu, J. Sun, Synthesis of gypsogenin and gypsogenic acid derivatives with antitumor activity by damaging cell membranes, New J. Chem. 43 (2019) 18898.

[26] H.I. Ciftci, M.O. Radwan, B. Sever, A.K. Hamdy, S. Emirdağ, N.G. Ulusoy, E. Sozer, M. Can, N. Yayli, N. Araki, H. Tateishi, M. Otsuka, M. Fujita, M.D. Altintop, EGFR-Targeted

Pentacyclic Triterpene Analogues for Glioma Therapy, Int. J. Mol. Sci. 22 (2021) 10945.

[27] H. Zhang, Y. Mu, F. Wang, L. Song, J. Sun, Y. Liu, J. Sun, Synthesis of gypsogenin derivatives with capabilities to arrest cell cycle and induce apoptosis in human cancer cells, R. Soc. Open Sci. 5 (2018) 171510.

[28] H.I. Ciftci, S.E. Ozturk, T.F.S. Ali, M.O. Radwan, H. Tateishi, R. Koga, Z. Ocak, M. Can, M. Otsuka, M. Fujita, The first pentacyclic triterpenoid gypsogenin derivative exhibiting anti-ABL1 kinase and anti-chronic myelogenous leukemia activities, Biol. Pharm. Bull. 41 (2018) 570-574.

[29] H.I. Ciftci, M.O. Radwan, S.E. Ozturk, N.G. Ulusoy, E. Sozer, D. Ellakwa, Z. Ocak, M. Can, T.F.S. Ali, H.I. Abd-Alla, N. Yayli, H. Tateishi, M. Otsuka, M. Fujita, Design, synthesis and biological evaluation of pentacyclic triterpene derivatives: Optimization of anti-ABL Kinase activity, Molecules. 24 (2019) 3535.

[30] A.F. Abdel-Magid, K.G. Carson, B.D. Harris, C.A. Maryanoff, R.D. Shah, Reductive amination of aldehydes and ketones with sodium triacetoxyborohydride. studies on direct and indirect reductive amination procedures, J. Org. Chem. 61 (1996) 3849-3862.

[31] A.F. Abdel-Magid, S.J. Mehrman, A review on the use of sodium triacetoxyborohydride in the reductive amination of ketones and aldehydes, Org. Process Res. Dev. 10 (2006) 971-1031.

[32] S. Flis, T. Chojnacki, Chronic myelogenous leukemia, a still unsolved problem: pitfalls and new therapeutic possibilities, Drug Des. Devel. Ther. 13 (2019) 825-843.

[33] S. Soverini, R. Bassan, T. Lion, Treatment and monitoring of Philadelphia chromosome-positive leukemia patients: recent advances and remaining challenges, J. Hematol. Oncol. 12 (2019) 39.

[34] A.B. da Rocha, R.M. Lopes, G. Schwartsmann, Natural products in anticancer therapy, Curr. Opin. Pharmacol. 1 (2001) 364-369.

[35] M. Huang, J.J. Lu, J. Ding, Natural products in cancer therapy: Past, present and future, Nat. Prod. Bioprospect. 11 (2021) 5-13.

[36] M. Singh, V. Ravichandiran, Y.P. Bharitkar, A. Hazra, Natural products containing olefinic bond: Important substrates for semi-synthetic modification towards value addition, Curr. Org. Chem. 24 (2020) 709-745.

[37] S. Lü, J. Wang, Homoharringtonine and omacetaxine for myeloid hematological malignancies, J. Hematol. Oncol. 7 (2014) 2.

[38] A. Bedi, B.A. Zehnbauer, J.P. Barber, S.J. Sharkis, R.J. Jones, Inhibition of apoptosis by BCR-ABL in chronic myeloid leukemia, Blood. 83 (1994) 2038-2044.

[39] J.L. Fernandez-Luna, Bcr-Abl and inhibition of apoptosis in chronic myelogenous leukemia cells, Apoptosis. 5 (2000) 315-318.

[40] M. Horita, E.J. Andreu, A. Benito, C. Arbona, C. Sanz, I. Benet, F. Prosper, J.L. Fernandez-Luna, Blockade of the Bcr Abl kinase activity induces apoptosis of chronic myelogenous leukemia cells by suppressing signal transducer and activator of transcription 5-dependent expression of Bcl-Xl, J. Exp. Med. 191 (2000) 977-984.

[41] K. Danisz, J. Blasiak, Role of anti-apoptotic pathways activated by BCR/ABL in the resistance of chronic myeloid leukemia cells to tyrosine kinase inhibitors, Acta Biochim. Pol. 60 (2013) 503-514.

[42] P. Seshacharyulu, M.P. Ponnusamy, D. Haridas, M. Jain, A.K. Ganti, S.K. Batra, Targeting the EGFR signaling pathway in cancer therapy, Expert Opin. Ther. Targets. 16 (2012) 15-31.

[43] M.L. Uribe, I. Marrocco, Y. Yarden, EGFR in cancer: Signaling mechanisms, drugs, and acquired resistance, Cancers (Basel). 13 (2021) 2748.

[44] A.A. Farooqi, Z.H. Siddik, Platelet-derived growth factor (PDGF) signalling in cancer: Rapidly emerging signalling landscape, Cell Biochem. Funct. 33 (2015) 257-265.

[45] S.W. Cowan-Jacob, G. Fendrich, A. Floersheimer, P. Furet, J. Liebetanz, G. Rummel, P. Rheinberger, M. Centeleghe, D. Fabbro, P.W. Manley, Structural biology contributions to the discovery of drugs to treat chronic myelogenous leukaemia, Acta Crystallogr. D Biol. Crystallogr. 63 (2007) 80-93.

[46] G. Van Den Driessche, D. Fourches, Adverse drug reactions triggered by the common HLA-B*57:01 variant: A molecular docking study, J. Cheminform. 9 (2017) 13.

[47] M. Oliverio, M. Nardi, M.L. Di Gioia, P. Costanzo, S. Bonacci, S. Mancuso, A. Procopio, Semi-synthesis as a tool for broadening the health applications of bioactive olive secoiridoids: A critical review, Nat. Prod. Rep. 38 (2021) 744.

[48] H. Tateishi, K. Monde, K. Anraku, R. Koga, Y. Hayashi, H.I. Ciftci, H. DeMirci, T. Higashi, K. Motoyama, H. Arima, M. Otsuka, M. Fujita, A clue to unprecedented strategy to HIV eradication: "Lock-in and apoptosis", Sci. Rep. 7 (2017) 8957.

[49] H.I. Ciftci, N. Bayrak, H. Yildirim, M. Yildiz, M.O. Radwan, M. Otsuka, M. Fujita, A.F. Tuyun, Discovery and structure-activity relationship of plastoquinone analogues as anticancer agents against chronic myelogenous leukemia cells, Arch. Pharm. (Weinheim). 352 (2019) 1900170.

[50] N. Bayrak, H. Yildirim, M. Yildiz, M.O. Radwan, M. Otsuka, M. Fujita, A.F. Tuyun, H.I. Ciftci, Design, synthesis, and biological activity of Plastoquinone analogs as a new class of anticancer agents, Bioorg. Chem. 92 (2019) 103255.

[51] H.I. Ciftci, N. Bayrak, M. Yıldız, H. Yıldırım, B. Sever, H. Tateishi, M. Otsuka, M. Fujita, A.F. Tuyun, Design, synthesis and investigation of the mechanism of action underlying anti-leukemic effects of the quinolinequinones as LY83583 analogs, Bioorg. Chem. 114 (2021) 105160.

[52] N. Bayrak, H.I. Ciftci, M. Yildiz, H. Yildirim, B. Sever, H. Tateishi, M. Otsuka, M. Fujita, A.F. Tuyun, Structure based design, synthesis, and evaluation of anti-CML activity of

the quinolinequinones as LY83583 analogs, Chem. Biol. Interact. 345 (2021) 109555.

[53] H. Ciftci, B. Sever, F. Ocak, N. Bayrak, M. Yıldız, H. Yıldırım, H. DeMirci, H. Tateishi, M. Otsuka, M. Fujita, A.F. TuYuN, *In vitro* and *in silico* study of analogs of plant product plastoquinone to be effective in colorectal cancer treatment, Molecules. 27 (2022) 693.

Table 1. The cytotoxic effects of compounds **6a-l** on K562 cells and PBMCs.

Compound	**IC_{50} value (µM)**		**SI***
	K562 cells	**PBMCs**	
6a	41.49±9.59		
6b	78.85±12.13		
6c	>100		
6d	>100		
6e	53.85±10.94		
6f	>100		
6g	>100		
6h	>100		
6i	>100		
6j	23.84±3.32		
6k	42.74±7.21		
6l	11.32±2.04	40.64±8.29	3.59
Imatinib	4.89±1.86	25.72±7.44	5.26

* SI= IC_{50} for PBMCs / IC_{50} for K562 cells.

Table 2. The cytotoxic effects of compounds **6a-l** on Jurkat, MT-2 and HeLa cells.

Compound	**IC_{50} value (μM)**		
	Jurkat cells	**MT-2 cells**	**HeLa cells**
6l	12.97±3.52	32.95±5.92	49.81±8.38
Imatinib	8.15±2.05	15.24±3.16	25.46±4.43

Table 3. Docking score (kcal/mol), glide gscore (kcal/mol) and glide emodel (kcal/mol) results of compounds **6a-l** in the ATP-binding cleft of Abl TK (PDB ID code: 2HYY).

Compound	**2HYY**		
	Docking score	**Glide score**	**Glide emodel**
6a	-3.624	-3.647	-43.975
6b	-3.564	-5.376	-67.175
6c	-4.920	-5.390	-62.445
6d	-4.382	-4.388	-44.286
6e	-3.829	-3.826	-46.362
6f	-4.002	-4.013	-58.553
6g	-4.261	-4.267	-46.780
6h	-4.042	-4.038	-31.718
6i	-3.773	-3.828	-42.062
6j	-5.927	-6.343	-65.644
6k	-5.183	-5.194	-69.733
6l	-6.021	-6.027	-43.263
Imatinib	-8.589	-11.093	-117.666

Table 4. Predicted pharmocokinetic properties of compound **6l** and imatinib.

Compound	QPlogBB* (-3 to 1.2)	CNS* (-2.0 to +2)	Human oral absorption%* (>80% is high, <25% is poor)	Rule of Five**	Rule of Three***
6a	-0.691	-1	85.378	2	1
6b	0.096	1	55.399	1	2
6c	-0.058	0	53.760	2	2
6d	-0.521	0	71.391	1	1
6e	-0.857	-1	80.025	2	1
6f	-1.857	-2	57.627	2	2
6g	-1.524	-2	72.524	2	1
6h	-0.449	-1	94.757	2	2
6i	-0.783	-1	89.600	2	1
6j	-0.874	-1	94.660	2	1
6k	-1.755	-2	68.646	2	1
6l	-0.773	-1	91.265	2	1

* QPlogBB: brain/blood partition coefficient, CNS**:** Predicted central nervous system activity, Percent Human-Oral Absorption: human oral absorption on 0-100% scale.

** Rule of Five: Number of violations of Lipinski's rule of five. The rules are: mol_MW (Molecular weight of the molecule) <500, QPlogPo/w (Predicted octanol/water partition coefficient) <5, donorHB (hydrogen-bond donor atoms) ≤ 5, accptHB (hydrogen-bond acceptor atoms) ≤ 10. Compounds that provide these rules are considered drug-like. (The "five" refers to the limits, which are multiples of 5).

*** Rule of Three: Number of violations of Jorgensen's rule of three. The three rules are: QPlogS (Predicted aqueous solubility)>-5.7, QPPCaco (Predicted apparent Caco-2 cell

permeability in nm/s)> 22 nm/s, # Primary Metabolites <7. Compounds with fewer (and preferably no) violations of these rules are more likely to be orally available agents (Schrödinger Release 2016-2: Schrödinger, LLC, New York, NY, USA).

Scheme 1. Obtaining of gypsogenin (**1**).

Scheme 2. The synthetic route for the preparation of compounds **6a-l**. Reagents and conditions: (i) $C_2H_4Cl_2$, amine derivatives; (ii) $NaBH(OAc)_3$, rt, 24 h.

Fig. 1. (**A**) First, second and third generation of TK inhibitors used in CML treatment and (**B**) some important natural Abl TK inhibitors.

Fig. 2. Gypsogenin derivatives, which were previously determined by our research group as potential Abl TK inhibitors.

Fig. 3. The diagram for spectral analysis of compounds **6a-l**.

Fig. 4. Changes in K562 cell line following exposure to IC_{50} concentration of compound **6l** and imatinib **(A)** for 6 h. The percentage of alive (blue), apoptosis (green), necrosis or late apoptosis (both green and red) and necrosis (red) cells **(B)** was quantified by analyzing 100 randomly chosen stained cells in each experiment. **(C)** Data from four independent experiments are shown as means ±SD, and *p* values were determined using Student's t test (ns: not statistically significant).

Fig. 5. The Abl TK inhibition of compound **6l** and imatinib at different concentrations. Data from three different experiments are shown as means ± standard deviations. P values were determined using Student's t test.

Fig. 6. The inhibition of a panel of tyrosine kinases by compound **6l** and imatinib at 30 µM concentration. Data from three different experiments are shown as means ± standard

deviations. P values were determined using Student's t test. (ns: not statistically significant).

Fig. 7. Docking poses of compounds **6a-l** and imatinib in the ATP-binding pocket of Abl TK (PDB code: 2HYY) (**A**) (surface presentation) (**B**) (ribbon presentation). (Yellow dashes: hydrogen bonding, green dashes: π-π interactions).

Fig. 8. Docking poses of compound **6l** and imatinib in the ATP-binding pocket of Abl TK (PDB code: 2HYY) (**A**) (surface presentation) (**B**) (ribbon presentation). (Yellow dashes: hydrogen bonding, green dashes: π-π interactions) (coloured in plum for compound **6l** and blue purple for imatinib).

Fig. 9. Docking pose interactions of compounds **6l, 6j** and imatinib in the ATP-binding pocket of Abl TK (PDB code: 2HYY).

Declaration of interests

☒ The authors declare that they have no known competing financial interests or personal relationships that could have appeared to influence the work reported in this paper.

☐ The authors declare the following financial interests/personal relationships which may be considered as potential competing interests:

Highlights

• New gypsogenin derivatives (**6a-l**) were synthesized *via* well-established synthetic procedures.

• Compound **6l** was found to have strongest cytotoxic effect on K562 chronic myelogenous leukemia (CML) cells compared to imatinib.

• Compound **6l** caused a significant apoptotic death of K562 cell line.

• Compound **6l** inhibited Abl tyrosine kinase (TK) significantly.

• Compound **6l** formed key interactions in the ATP-binding pocket of Abl TK.

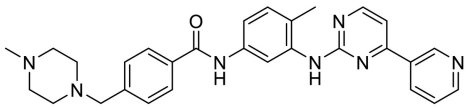

Imatinib

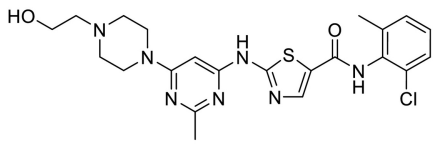

Dasatinib

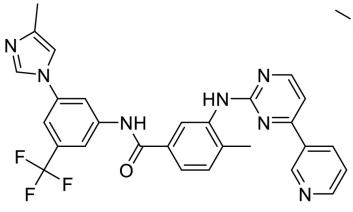

Nilotinib

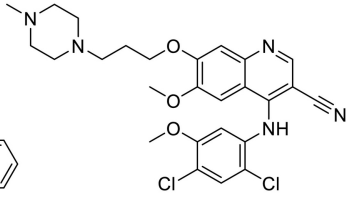

Bosutinib

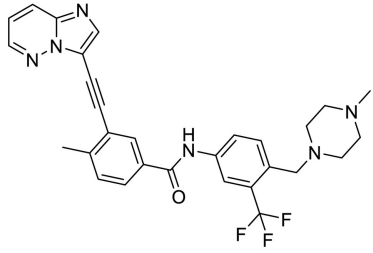

Ponatinib

(A)

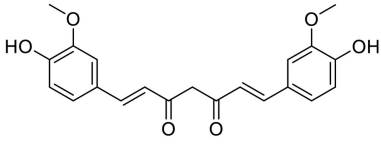

Curcumin

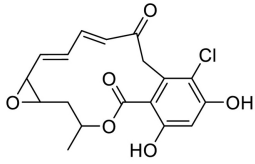

Radicicol

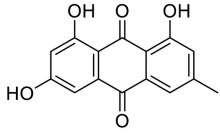

Emodin

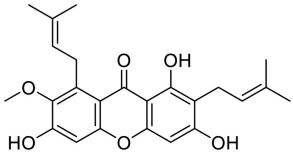

α-Mangostin

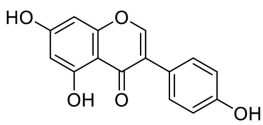

Genistein

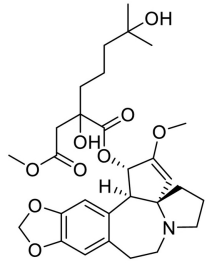

Homoharringtonine

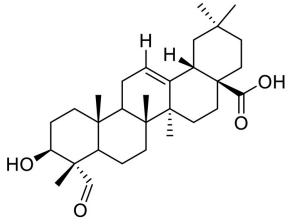

Gypsogenin

(B)

Figure 1

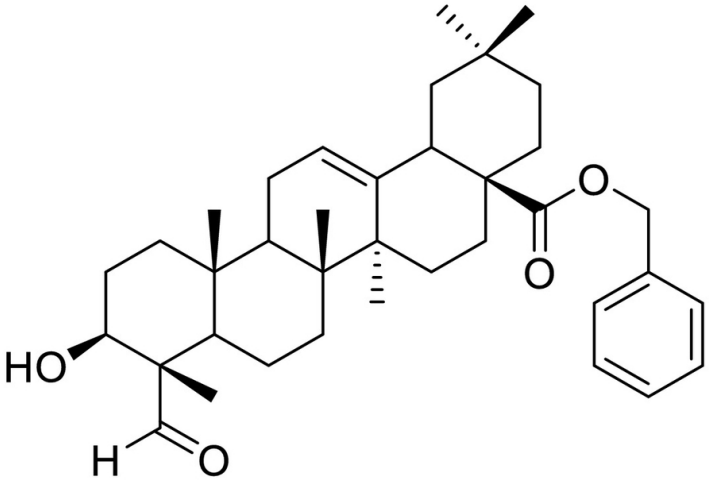

Compound **1c**

K562 CML cell line IC_{50}= 9.3 μM

Abl TK inhibition IC_{50}= 8.7 μM

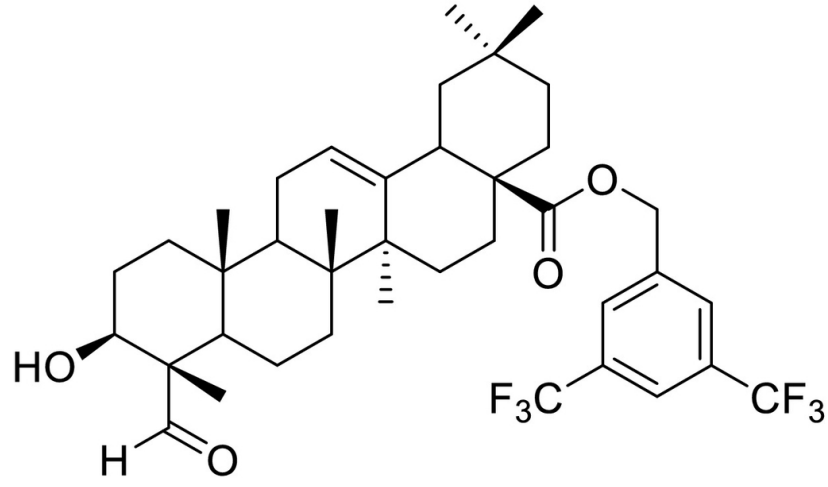

Compound **GP2**

K562 CML cell line IC_{50}= 4.78 μM

Abl TK inhibition IC_{50}= 7.19 μM

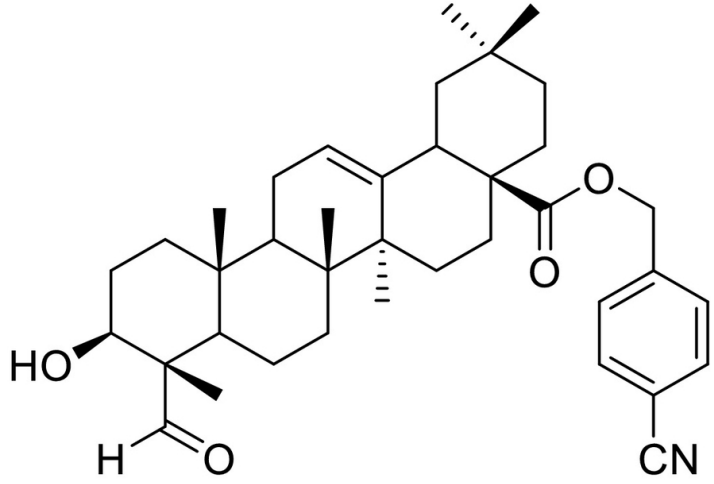

Compound **GP5**

K562 CML cell line IC_{50}= 3.19 μM

Abl TK inhibition IC_{50}= 6.16 μM

Figure 2

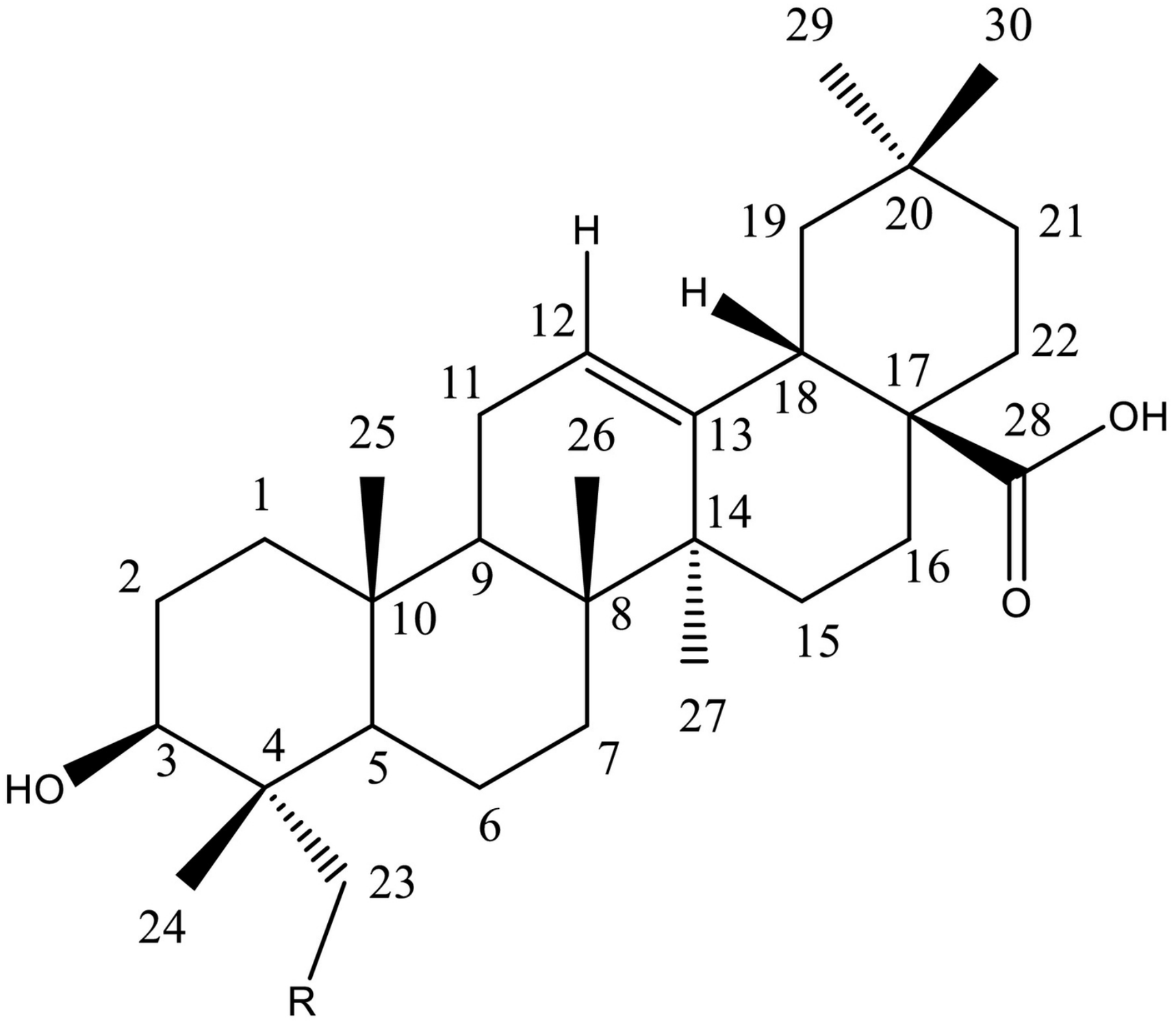

Compounds **6a-l**

Figure 3

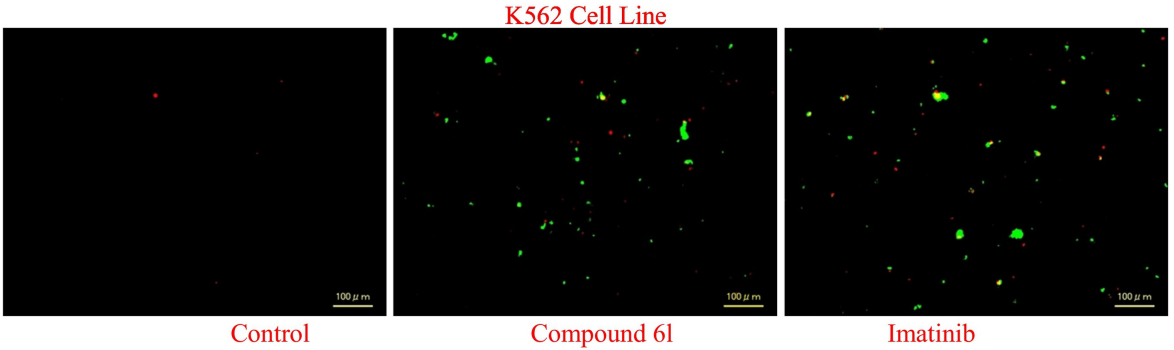
K562 Cell Line
100 μm
100 μm
100 μm
Control
Compound 6l
Imatinib

A

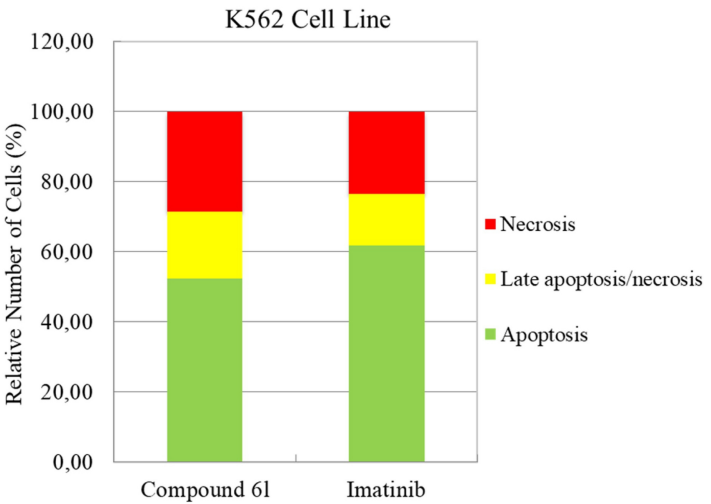
K562 Cell Line
Relative Number of Cells (%)
120,00
100,00
80,00
60,00
40,00
20,00
0,00
Compound 6l
Imatinib
Necrosis
Late apoptosis/necrosis
Apoptosis

B

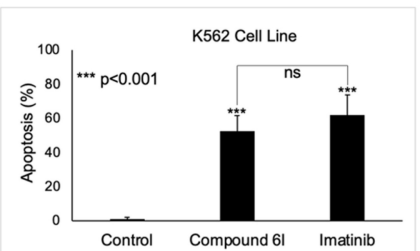
K562 Cell Line
Apoptosis (%)
100
80
60
40
20
0
*** p<0.001
ns
***
***
Control
Compound 6l
Imatinib

C

Figure 4

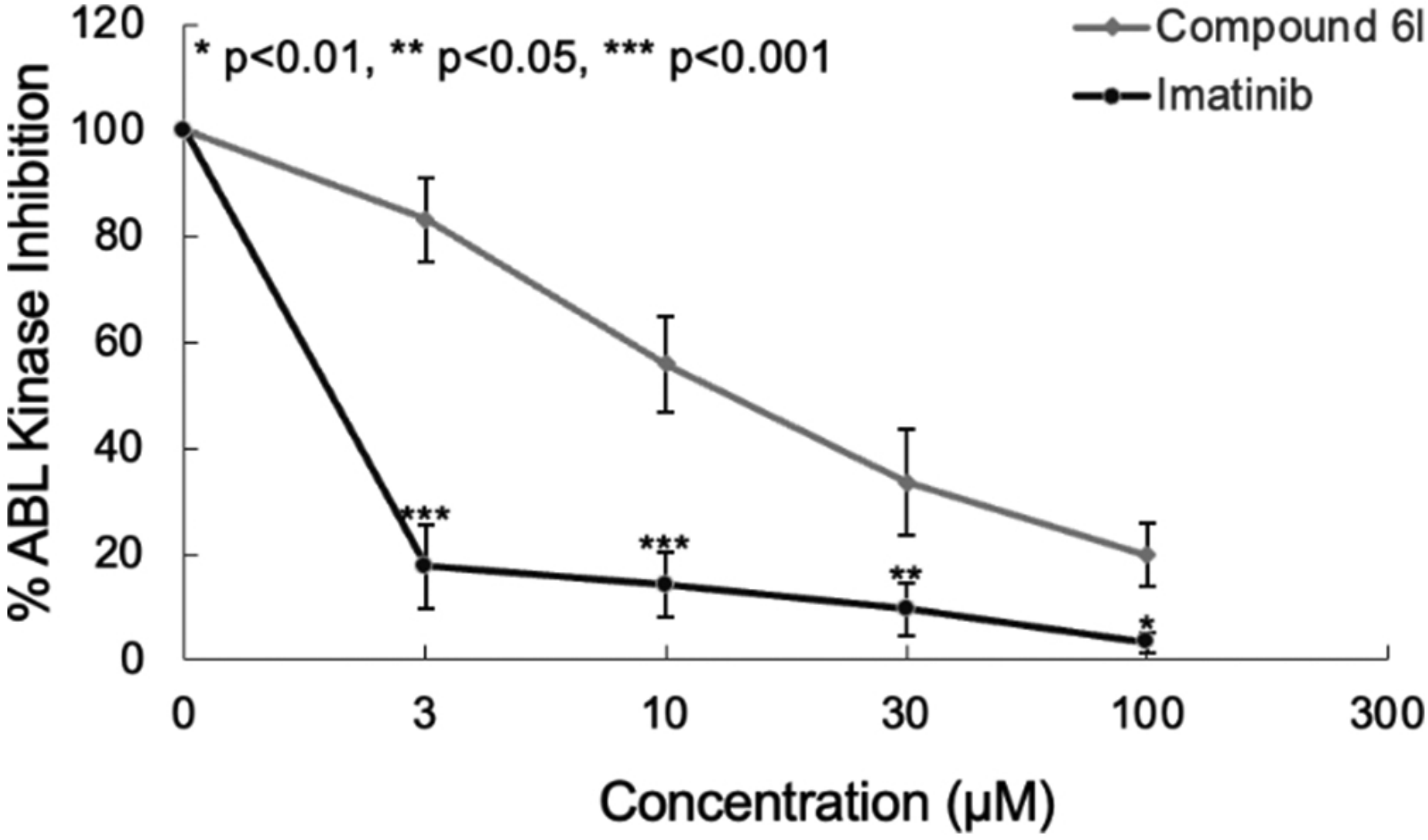
* p<0.01, ** p<0.05, *** p<0.001
Compound 6l
Imatinib
% ABL Kinase Inhibition
120
100
80
60
40
20
0
***
***
**
*
0
3
10
30
100
300
Concentration (μM)

Figure 5

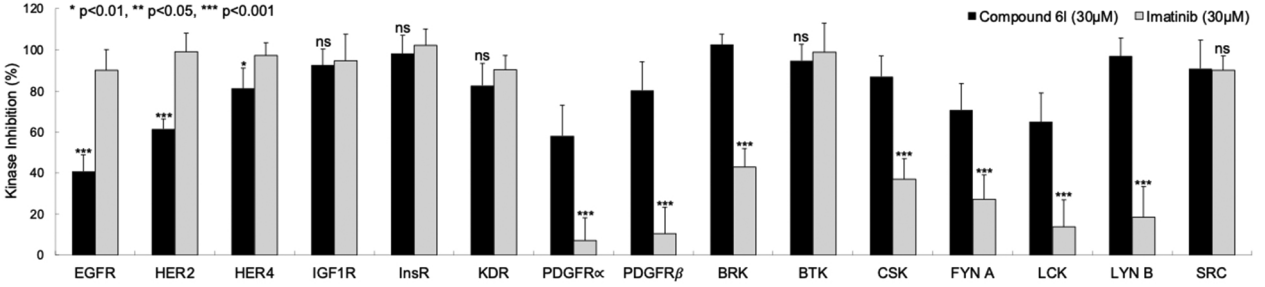
* p<0.01, ** p<0.05, *** p<0.001
Compound 6l (30μM)
Imatinib (30μM)
Kinase Inhibition (%)
120
100
80
60
40
20
0
EGFR
HER2
HER4
IGF1R
InsR
KDR
PDGFRα
PDGFRβ
BRK
BTK
CSK
FYN A
LCK
LYN B
SRC
ns
*
***

Figure 6

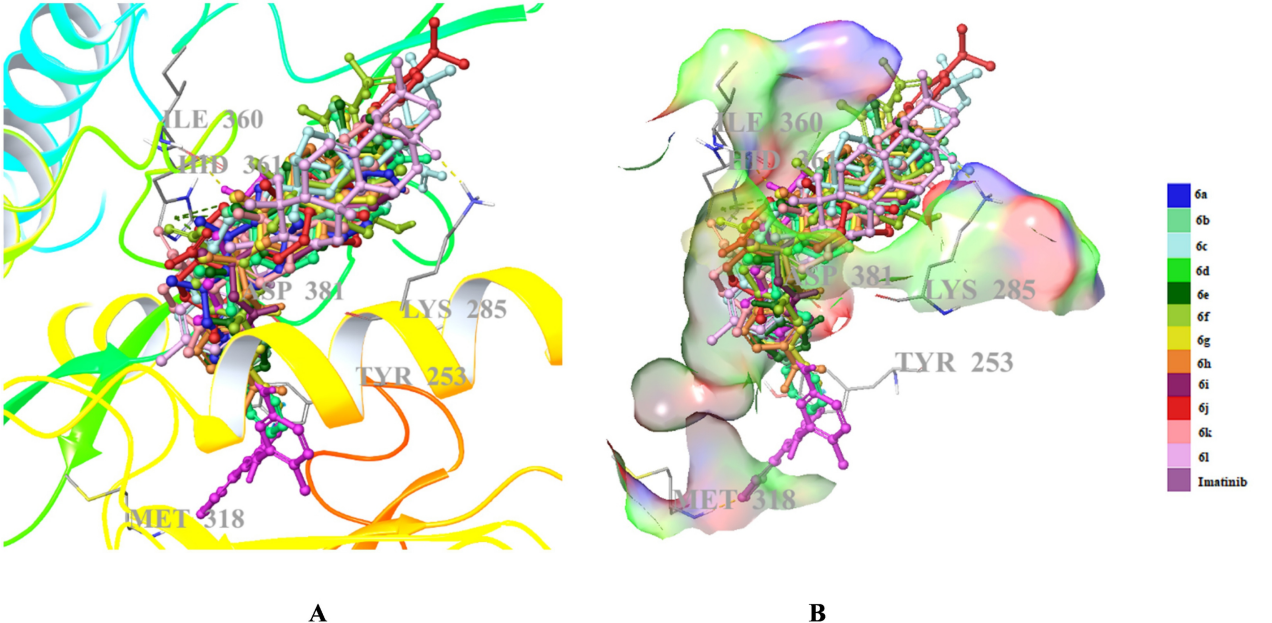
ILE 360
HIS 361
ASP 381
LYS 285
TYR 253
MET 318
ILE 360
ASP 381
LYS 285
TYR 253
MET 318
6a
6b
6c
6d
6e
6f
6g
6h
6i
6j
6k
6l
Imatinib

A **B**

Figure 7

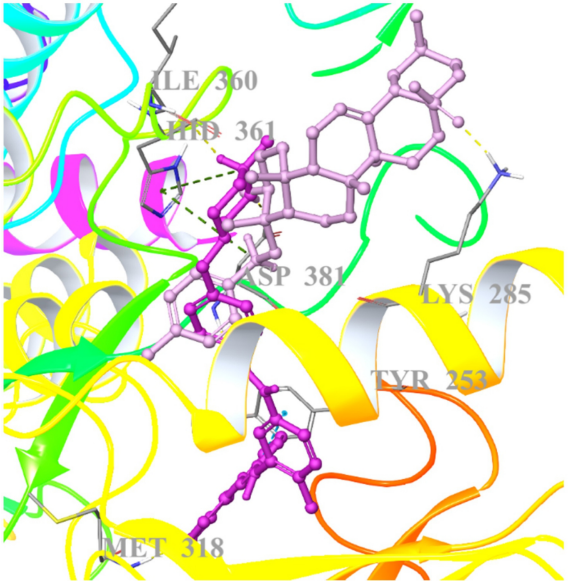
ILE 360
HID 361
ASP 381
LYS 285
TYR 253
MET 318

A

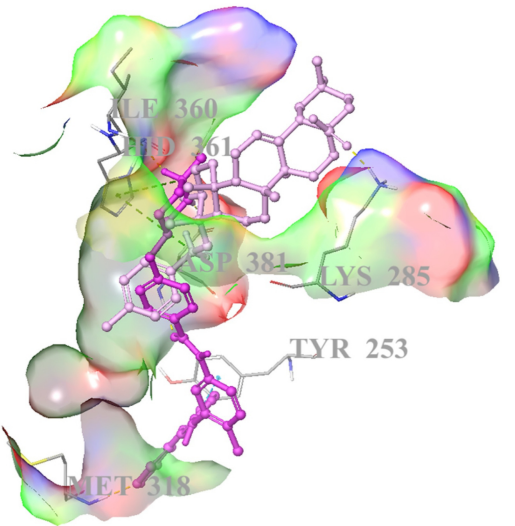
ILE 360
HID 361
ASP 381
LYS 285
TYR 253
MET 318

B

Figure 8

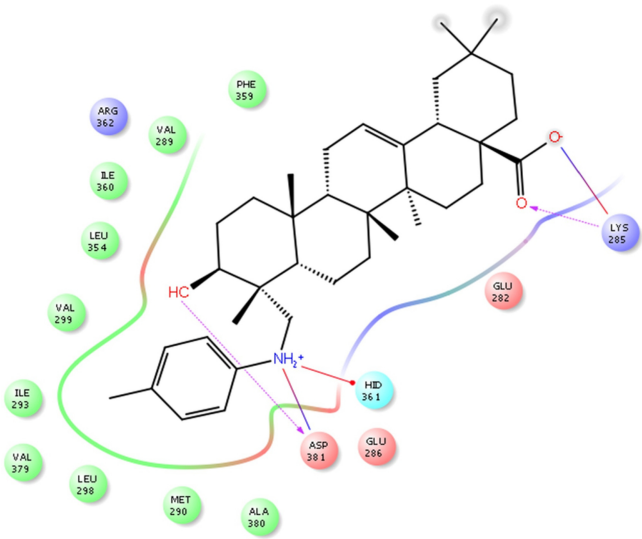

Compound **6l**

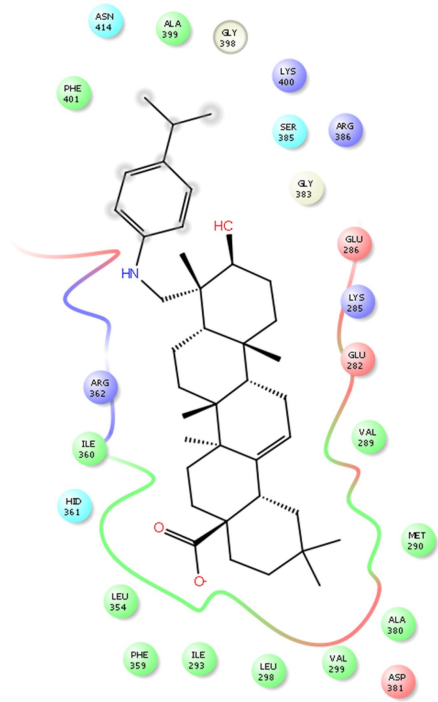

Compound **6j**

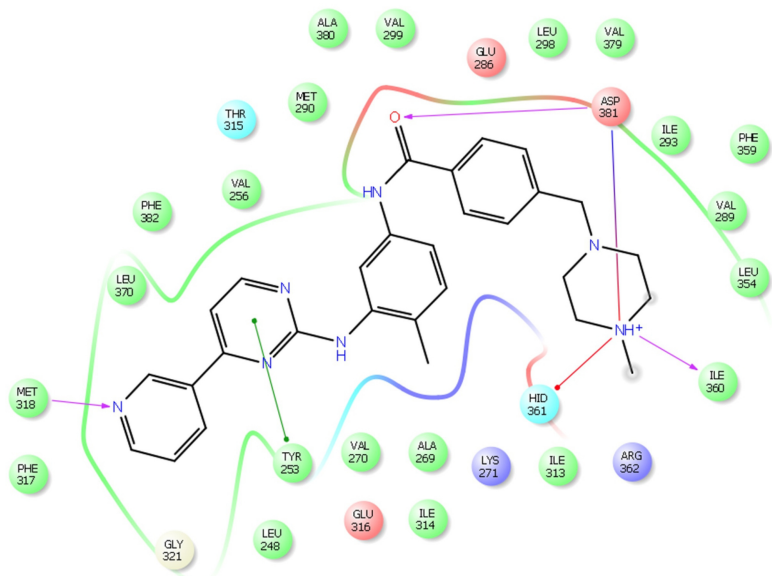

Imatinib

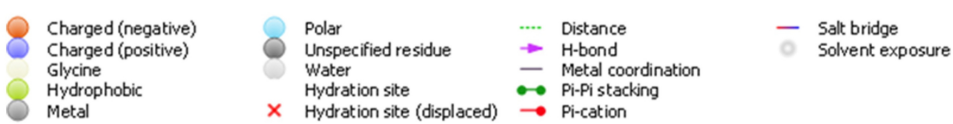

Figure 9